GENETICS, 2026, iyag112
https://doi.org/10.1093/genetics/iyag112
Advance Access Publication Date: 29 May 2026
Neurogenetics

Amyloid precursor protein ortholog Appl acts with Vnd during mushroom body axon growth in *Drosophila*

Claire Marquilly,[1,7] Germain U. Busto,[1,8] Laure Pasquer,[2] Robert P. Zinzen,[3] Bassem A. Hassan,[4] Lee G. Fradkin,[5] Thomas Preat,[2] Ana Boulanger,[1,6] Jean-Maurice Dura [1,*]

[1]IGH, Univ Montpellier, CNRS, 141 rue de la Cardonille, Montpellier 34396, France
[2]Brain Plasticity Unit, CNRS, ESPCI Paris, PSL Research University, 10 rue Vauquelin, Paris 75005, France
[3]Max Delbrück Centrum für moleculare Medizin in der Helmholtz Gemeinschaft (MDC), BIMSB, Robert-Rössle-Straβe 10, Berlin 13125, Germany
[4]Institut du Cerveau-Paris Brain Institute (ICM), Sorbonne Université, Inserm, CNRS, Hôpital Pitié-Salpêtrière, 47 Boulevard de l'Hôpital, Paris 75013, France
[5]Institute for Stem Cell Biology and Regenerative Medicine, Lokey Stem Cell Research Building (SIM1), Stanford University Medical School, Stanford University, 265 Campus Drive, 3rd Floor, Stanford, CA 94305, United States
[6]Institute of Functional Genomics (IGF), University of Montpellier, CNRS, INSERM, 141 rue de la Cardonille, Montpellier 34396, France
[7]Present address: Centre for Research in Neuroscience, Research Institute of the McGill University Health Centre, 1650 Cedar Ave., L12-401, Montreal, QC, Canada H3G 1A4
[8]Present address: INM, Univ Montpellier, INSERM, 80 avenue Augustin Fliche, Montpellier 34091, France

*Corresponding author: IGH, Univ Montpellier, CNRS, 141 rue de la Cardonille, Montpellier 34396, France. Email: jean-maurice.dura@igh.cnrs.fr

The amyloid precursor protein (APP) is associated with Alzheimer's disease. *Appl* is the single *Drosophila* APP ortholog and is expressed in all neurons throughout development. Appl was previously shown to cell-autonomously modulate axon outgrowth in the mushroom bodies (MBs), the fly olfactory memory center. However, we found that $Appl^{d}$, the only reported null allele, affects the normal function of *vnd*, the gene just proximal to *Appl*. To decipher developmental and memory defects specifically due to a loss of only *Appl* function, we generated a precise *Appl* null allele ($Appl^{C2.1}$) by CRISPR/Cas9 genomic engineering. With $Appl^{C2.1}$, we confirmed the partial contribution for *Appl* in MB axon outgrowth. We also produced new CRISPR *vnd* alleles removing either *vnd-B* or *vnd-A* function. We report here that *vnd* is also required for MB β-branch axon outgrowth and to a much greater extent than *Appl* itself. Moreover, *vnd* is expressed in neurons close to, but not within, the MB during development and is required non-cell-autonomously for MB axon outgrowth. It was previously shown that *Appl* knockdown in the MBs results in loss of memory following the association of odorants with electric shocks. Differently from $Appl^{d}$ flies we found no defects of electric shock avoidance in $Appl^{C2.1}$ flies, allowing us to test for memory. $Appl^{C2.1}$ flies showed a complete loss of long-term memory which was fully rescued by MB-restricted expression of $Appl^{+}$ only during the adult stage. Therefore, we demonstrate that the complete lack of Appl affects memory independently from structural developmental defects.

Keywords: CRISPR; Appl null; Vnd-A null; Vnd-B null; brain development; mushroom body; axon growth; Vnd-Appl signaling; aversive long-term memory

Introduction

Alzheimer's disease (AD) is associated with extracellular accumulation of amyloid fibrils derived from the amyloid precursor protein (APP). APPs have therefore been intensely investigated, however their physiological function in the brain remains unclear and controversial (Nicolas and Hassan 2014; Soldano and Hassan 2014; Selkoe and Hardy 2016). Although there are 3 paralogues in mammals (APP, APLP1, and APLP2), *Drosophila* encodes a single APP homologue, called *Appl*, that is expressed in all neurons throughout development (Martin-Morris and White 1990). It has been shown that the type I transmembrane protein coding gene *Appl* is a conserved neuronal modulator of a Wnt planar cell polarity (Wnt/PCP) pathway, a regulator of cellular orientation within the plane of an epithelium (Soldano et al. 2013). It has been proposed that Appl is part of the membrane complex formed by the core PCP receptors Fz (*frizzled*) and Vang (*Van Gogh*) required for axon growth (Soldano et al. 2013; Liu et al. 2021).

The mushroom bodies (MBs) are 2 bilaterally symmetric structures in the central brain that are required for learning and memory (Lin 2023). Each MB is comprised of 2,000 neurons that arise from 4 neuroblasts. Three types of neurons appear sequentially during development: the embryonic/early larval γ, the larval α′β′, and the late larval/pupal αβ types. Each αβ neuron projects an axon that branches to send an α branch dorsally, which contributes to the formation of the α lobe, and a β branch medially, which contributes to the formation of the β lobe (Lee et al. 1999). Appl's expression continues in adult flies, notably in the MB αβ neurons (Leyssen et al. 2005; Rabah et al. 2025). So far, $Appl^{d}$ is the only reported null *Appl* allele and it results from a synthetic genomic deletion removing the *Appl* locus (Luo et al. 1992). The $Appl^{d}$-bearing chromosome was selected, after γ irradiation, as a translocation of a partial duplication of the X chromosome on the Y chromosome to a X chromosome terminal deficiency (Supplementary Fig. 1). $Appl^{d}$ flies are viable, fertile and display no gross structural defects in the brain (Luo et al. 1992). However, the *Appl* signaling pathway is required for proper axon outgrowth in the MBs since $Appl^{d}$ flies display modestly penetrant axonal defects in αβ neurons. Importantly, Appl is required

Received on 23 July 2025; accepted on 07 April 2026

cell-autonomously for β-branch axon outgrowth (Soldano et al. 2013; Cassar and Kretzschmar 2016).

The *ventral nervous system defective* (*vnd*) gene, which is immediately proximal to *Appl*, encodes a Nk2-class homeodomain transcription factor, that acts in a context-dependent manner as an activator or repressor and is essential for the development of the nervous system. The *vnd* gene encodes 2 proteins: Vnd-A and Vnd-B whose mRNAs arise from 2 different promoters. These 2 proteins differ in their aminoterminal domains and are identical in the remainder of their sequences. While Vnd-A is a transcription repressor for promoters containing Nk-2 binding sites, Vnd-B directly activates transcription, also likely via binding to the same binding site. (Stepchenko et al. 2011). Flies bearing a null allele of vnd in hemi- or homozygous condition die during embryogenesis (Jiménez et al. 1995).

We found that the $Appl^{d}$ chromosome also genetically affects *vnd* function. To genetically dissect *Appl* and *vnd* functions, we generated CRISPR alleles that precisely delete the *Appl* gene without affecting *vnd* function ($Appl^{C2.1)}$ and that precisely delete each 1 of the 2 *vnd* transcripts without affecting *Appl* ($vnd^{C\Delta A}$ and $vnd^{C\Delta B}$). To analyze the exact developmental and memory defects due to the specific loss of the *Appl* function only, we used $Appl^{C2.1}$ and first confirmed the partial contribution of *Appl* in MB β-branch axon outgrowth. We showed here that *vnd*-A, but not *vnd-B*, is also required for MB β-branch axon outgrowth. Unexpectedly, *vnd* is expressed in neurons close to, but not within, the MB during development and is required non-cell-autonomously, likely by promoting the production of a secreted factor(s) involved in the MB axon outgrowth. Interestingly, $Appl^{C2.1}$ flies, in contrast to $Appl^{d}$ flies, showed a normal response to electric shock but a complete loss of long-term memory (LTM) of that shock independently from potential brain development defects.

Materials and methods

Drosophila stocks

All crosses were performed on standard culture medium at 25 °C. Except where otherwise stated, all alleles and transgenes have been described previously (http://flystocks.bio.indiana.edu/). The following alleles were used: $Appl^{C1.4}$, $Appl^{C2.1}$, $vnd^{C\Delta A}$, and $vnd^{C\Delta B}$ were generated in this study. *Appl*-y^{+} (BL #56073), $Appl^{d}$ (BL #43632), vnd^{A} (BL #57139), $vnd^{\Delta 38}$ (Chu et al. 1998), vnd^{6} (Jiménez et al. 1995). The following transgenes were used: *UAS-mCD8::GFP* (BL #5137), *UAS-Appl* (BL #38403) and the duplications resulting from genomic transgenes *Dp(1;3) DC430* (BL #32288) and *Dp(1.3) DC009* (BL #30219) which are both inserted into the same attP site at 65B2. For simplicity, we refer to *Dp(1;3) DC430* as *Dp-Appl*$^{+}$ and *Dp(1.3) DC009* as *Dp-vnd*$^{+}$. *Dp-Appl*$^{+}$ is ~97 kb and contains 11 genes including the *Appl* gene but not the *vnd* gene. *Dp-vnd*$^{+}$ is also ~97 kb and contains 15 genes including the *vnd* gene but not the *Appl* gene. We used 3 GAL4 lines: *vnd-T2A-GAL4* (Lee et al. 2020) which reveals *vnd* transcription, *c739-GAL4* (BL #7362) expressed in adult αβ MB neurons (Aso et al. 2009) and VT30559 expressed in adult MB neurons (Placais et al. 2017). Recombinant chromosomes were obtained by standard genetic procedures. In the case of the recombination between y^{+} and $Appl^{C2.1}$ (~170 kb apart) we screened for [y^{+}] viable males coming from y^{+} $vnd^{\Delta 38}$/y $Appl^{C2.1}$ females. Note that $vnd^{\Delta 38}$ is an embryonic lethal mutation. Four [y^{+}] viable males out of 11,320 males were obtained. One male was sterile, but 3 y^{+} $Appl^{C2.1}$/Y males gave progeny (percentage of recombination ~0.027%) and were confirmed by genomic Polymerase Chain Reaction (PCR). Note that the *Appl* mutant phenotypes were observed in a recent outcrossed Canton-S genetic background. MARCM stocks: *tubP-GAL80*, *hsFLP122*, *hsFLP1*, *FRT19A* (all on the X chromosome).

CRISPR-Cas9 strategy

All guide RNA sequences (single guide RNA [sgRNA]) were selected using the algorithm (http://targetfinder.flycrispr.neuro.brown.edu/) containing 20 nucleotides each (PAM excluded) and are predicted to have zero off-targets. We selected 1 pair of sgRNA for the *Appl* gene and 2 pairs of sgRNA for the *vnd* gene. For *Appl*, the pair is targeting the entire transcriptional unit. For *vnd*, each pair is targeting either the A specific region of *vnd* or the B specific region of *vnd*. We used the following oligonucleotide pairs: CRISPR-1 Appl fwd and CRISPR-1 Appl rev to target the all *Appl* region, CRISPR-1 vnd A fwd and CRISPR-1 vnd A rev to target the A region of *vnd*, CRISPR-1 vnd B fwd and CRISPR-1 vnd B rev to target the B region of *vnd* (see the corresponding oligonucleotide sequences in Supplementary Material). We introduced 2 sgRNA sequences into pCFD4 (Port et al. 2014), a gift from Simon Bullock (Addgene plasmid #49411) by Gibson Assembly (New England Biolabs) following the detailed protocol at crisprflydesign.org. For PCR amplification, we used the protocol described on that website. Construct injection was performed by BestGene (Chino Hills, CA, USA) and all the transgenes were inserted into the same attP site (VK00027 at 89E11). Being aware that the DNA excision of nearly 50 kb might be rare, we have decided to use a positive screen before validation by genomic PCR. We have used a stock where the *Appl* gene is marked by a y^{+} construct. The deletion of the *Appl* gene should therefore be associated to y^{-} phenotype. Transgenic males expressing the *Appl* sgRNAs and bearing an isogenized X chromosome (*y Appl-y*$^{+}$ *Act-Cas9 w**) were crossed to *FM7c/ph*^{0} *w* females. One hundred and eighty crosses were set up and only 2 crosses gave rise to y $Appl^{deletion?}$ *Act-Cas9 w*/FM7c* females indicating 1% of CRISPR efficacy. From each of these 2 crosses, a single y $Appl^{deletion}$ *Act-Cas9 w*/FM7c* female was crossed with *FM7c* males to make a stock ($Appl^{C1.4}$ and $Appl^{C2.1}$ where Cas9 was removed). The deletion was then validated by genomic PCR using 2 pairs of primers: $Appl^{C1.4}$ fwd (GAGCCAGATACAC AAGCACA)/$Appl^{C1.4}$ rev (GGCTTTGTTTACTTCCTGGC) and $Appl^{C2.1}$ fwd (TCCTACTACGTTCCACAATC)/$Appl^{C2.1}$ rev (TAATG CCCAACATATCCAAC). The precise endpoints of the deletion were determined by sequencing (Genewiz, France). Transgenic males expressing the different *vnd* sgRNAs were crossed to y *nos-Cas9 w** females bearing an isogenized X chromosome. One hundred crosses were set up for each sgRNA pair, with up to 5 males (because of poor viability) containing both the sgRNAs and *nos-Cas9*, and 5 *FM7c/ph*^{0} *w* females. From each selected cross, a single y $vnd^{deletion?}$ *nos-Cas9 w*/FM7c* female was crossed with *FM7c* males to make a stock which was validated for the presence of an indel by genomic PCR with primers flanking the anticipated deletion and the precise endpoints of the deletion were determined by sequencing (Genewiz) using *vnd*-specific primers: $vnd^{C\Delta A}$ fwd (ccaacaaagccgagagtctct)/$vnd^{C\Delta A}$ rev (cgggaatttctaagccagggt) and $vnd^{C\Delta B}$ fwd (cgatttggggcgttgtgagta)/$vnd^{C\Delta B}$ rev (gttgggctttaatccgggagt). A CRISPR efficacy of at least 5% was obtained in both cases. We kept a single stock from each set of CRISPR experiment: $vnd^{C\Delta A}$ and $vnd^{C\Delta B}$ where Cas9 was removed.

Brain dissection, immunostaining and MARCM mosaic analysis

Adult fly heads and thoraxes were fixed for 1 h in 3.7% formaldehyde in phosphate-buffered saline (PBS) and brains were dissected in PBS. For larval and pupal brains, brains were first dissected in PBS and then fixed for 15 min in 3.7% formaldehyde in PBS.

They were then treated for immunostaining as described (Lee and Luo 1999; Boulanger et al. 2011). Antibodies, obtained from the Developmental Studies Hybridoma Bank, were used at the following dilutions: mouse monoclonal anti–Fas2 (1D4) 1:10, mouse monoclonal anti-Repo (8D1.2) 1:10, mouse monoclonal anti-Elav (9F8A9) 1:1,000 and guinea pig polyclonal anti-vnd (1/1,000). Goat secondary antibodies conjugated to Cy3 against mouse or guinea pig IgG (Jackson ImmunoResearch Laboratory) were used at 1:300 for detection. DAPI (4', 6-diamidino-2-phénylindol) (Sigma) was used after secondary antibody washes. Tissues were incubated for 10 min at room temperature in a 1/1,000 solution from a stock containing 1 mg/mL of DAPI solution, then washed. To generate clones in the MB, we used the MARCM technique (Lee and Luo 1999). First instar larvae were heat-shocked at 37 °C for 1 h. Adult brains were fixed for 15 min in 3.7% formaldehyde in PBS before dissection and GFP (Green Fluorescent Protein) visualization.

Production of the anti-Vnd antiserum

Full length vnd-RA was amplified via PCR from cDNA and cloned into a pRSET bacterial expression vector (ThermoFisher) in frame with an N-terminal 6x-His tag, amplified in DH5alpha and transformed into BL21 competent cells for protein production. His-tagged VndA was purified over a Nickel-NTA agarose resin (Qiagen) according to manufacturer's recommendation. Purified protein was injected into guinea pigs by Squarix GmbH (Marl, Germany, www.squarix.de), selected by determining that pre-immunization sera did not produce signal in Western blots of fly extracts. Successive bleeds were screened for distinct signal in Western blots using embryo extracts and by immunohistochemistry, where signal was expected post 2.5 h AED (After Embryonic Development).

Microscopy and image processing

Images were acquired at room temperature using a Zeiss LSM 780 equipped with a 40× PLAN apochromatic 1.3 oil-immersion differential interference contrast objective lens and a Leica SP8 laser scanning confocal microscopes (MRI Platform, Institute of Human Genetics, Montpellier, France). The immersion medium used was Immersol 518F. The acquisition software used was Zen 2011 (black edition) for the Zeiss and LasX for the Leica. Contrast and relative intensities of the green (GFP), of the red (Cy3) and of the DAPI channels were processed with ImageJ (Fiji) software. Settings were optimized for detection without saturating the signal.

Quantitation of Vnd immunolabeling

For Vnd signal quantification, we used ImageJ software and performed an average of 8 measurements per VNC (Ventral Nerve Cord) from series of neuron pairs located along the center of the VNC. These neuronal groups are easily identifiable due to their consistent position and strong staining, enabling quantification of the same neuronal subtype within a VNC that contains a large number of labeled neurons. The mean of these measurements was then calculated for each sample. For graphical representation, data were normalized to 1 by dividing each value by the mean of the corresponding control. Within each independent experiment, groups of genotypes were processed simultaneously using the same antibody mix. Images were acquired using identical confocal settings within each experimental set, and all data were processed in parallel. Each experiment was repeated twice.

Behavior experiments

For behavior experiments, flies were raised on standard medium at 18 °C and 60% humidity in a 12-h light/dark cycle. We used the TARGET system (McGuire et al. 2003) to inducibly express UAS-*Appl*$^{+}$ construct exclusively in adult flies and not during development. Zero to 3-d old flies were transferred to fresh bottles containing standard medium and kept at 30.5 °C for 2 d before conditioning. For non-induced experiments, flies were transferred to fresh bottles containing standard medium and kept at 18 °C before conditioning. All the behavior experiments, including the sample sizes, were conducted similarly to other studies (de Tredern et al. 2021). Groups of 20 to 50 flies were subjected to olfactory conditioning protocol consisting of 5 associative cycles spaced by 15 min inter-trial intervals (5× spaced training). Conditioning was performed at 25 °C using previously described barrel-type machines that allow the parallel training of up to 6 groups (Pascual and Préat 2001). Throughout the conditioning protocol, each barrel was plugged into a constant air flow at 2 L/min. For a single cycle of associative training, flies were first exposed to an odorant (the CS+) for 1 min while 12 pulses of 5 s long 60 V electric shocks were delivered; flies were then exposed 45 s later to a second odorant without shocks (the CS^{-}) for 1 min. The odorants 3-octanol (Fluka 74878, Sigma-Aldrich) and 4-methylcyclohexanol (Fluka 66360, Sigma-Aldrich), diluted in paraffin oil to a final concentration of 2.79×10^{-1} g/L, were alternately used as conditioned stimuli. During unpaired conditionings, the odor and shock stimuli were delivered separately in time, with shocks occurring 3 min before the first odorant. Flies were kept at 18 °C on standard medium between conditioning and the memory test. The memory test was performed at 25 °C in a T-maze apparatus (Tully and Quinn 1985) 24 h after spaced training. Each arm of the T-maze was connected to a bottle containing 3-octanol and 4-methylcyclohexanol, diluted in paraffin oil to a final concentration identical to the 1 used for conditioning. Flies were given 1 min to choose between either arm of the T-maze. A performance score was calculated as the number of flies avoiding the conditioned odor minus the number of flies preferring the conditioned odor, divided by the total number of flies. A single performance index value is the average of 2 scores obtained from 2 groups of genotypically identical flies conditioned in 2 reciprocal experiments, using either odorant (3-octanol or 4-methylcyclohexanol) as the CS^{+}. The indicated "n" is the number of independent performance index values for each genotype. The shock response tests were performed at 25 °C by placing flies in 2 connected compartments; electric shocks were provided in only one of the compartments. Flies were given 1 min to move freely in these compartments, after which they were trapped, collected, and counted. The compartment where the electric shocks were delivered was alternated between 2 consecutive groups. Shock avoidance was calculated as for the memory test. Because the delivery of electric shocks can modify olfactory acuity, our olfactory avoidance tests were performed at 25 °C on flies that had first been presented with another odor paired with electric shocks. Innate odor avoidance was measured in a T-maze similar to those used for memory tests, in which 1 arm of the T-maze was connected to a bottle with odor diluted in paraffin oil and the other arm was connected to a bottle with paraffin oil only. Naive flies were given the choice between the 2 arms for 1 min. The odor-interlaced side was alternated for successively tested groups. Odor concentrations used in this assay were the same as for the memory assays. At these concentrations, both odorants are innately repulsive.

Statistics

Comparison between 2 groups expressing a qualitative variable was analyzed for statistical significance using the χ^2 test or the Fisher exact test. (BiostaTGV: http://biostatgv.sentiweb.fr/?module=tests). Comparison of 2 groups expressing a quantitative variable was analyzed using the 2-sided nonparametric Mann–Whitney *U* test. Graphs were created using GraphPad Prism software (version 10.5.0). For behavior experiments, all data are presented as mean ± SEM. Two groups of about 30 flies were reciprocally conditioned, using respectively octanol or methylcyclohexanol as the CS^+. The memory score was calculated from the performance of 2 groups as described above, which represents a single experimental replicate. Comparisons of the data series between 2 conditions were achieved by a 2-tailed unpaired *t*-test. Comparisons between more than 2 distinct groups were made using a 1-way ANOVA test, followed by Tukey pairwise comparisons between the experimental groups and their controls. ANOVA results are presented as the value of the Fisher distribution $F(x,y)$ obtained from the data, where x is the number of degrees of freedom between groups and y is the total number of degrees of freedom for the distribution. In the figures, asterisks illustrate the significance level of the *t*-test, or of the least significant pairwise comparison following an ANOVA. Values of $P < 0.05$ were considered to be significant. Statistical significance was defined as: ns = not statistically different, $^*P < 0.05$, $^{**}P < 0.01$, and $^{****}P < 0.0001$.

Results

Generating new *Appl* CRISPR alleles

The complex chromosome structure resulting in the $Appl^d$ allele complicates its subsequent genetic manipulation and might be a reason for the sensitivity of its phenotype to genetic background (Supplementary Fig. 1). Therefore, we produced new null *Appl* alleles by removing the entire *Appl* transcriptional unit via CRISPR/Cas9-mediated deletion (Doudna and Charpentier 2014). We recovered $Appl^{C1.4}$ and $Appl^{C2.1}$, 2 CRISPR *Appl* null alleles (Fig. 1a and Supplementary Fig. 2), following an adaptation of a published protocol to produce ~50 kb deletions (Port et al. 2014). $Appl^d$ MBs display a modestly penetrant cell-autonomous axon growth defect of the β-branches which manifests as an absence of the β lobe (Soldano et al. 2013; Liu et al. 2021).

Surprisingly, we found a strong difference in the penetrance of the absence of the β lobe phenotype in the 2 *Appl* CRISPR alleles. Although 9% of $Appl^{C2.1}$ MBs lacked the β lobe, slightly lower than the 14.5% described for $Appl^d$ (Marquilly et al. 2021), $Appl^{C1.4}$ MBs displayed a much higher penetrance (66%) of this phenotype (Fig. 1, b to d). We determined the extents of the precise deletions present in the 2 alleles via sequencing of PCR amplicons and found that while the $Appl^{C2.1}$ deletion precisely removed the *Appl* transcriptional unit, the $Appl^{C1.4}$ allele also removed a part of the *vnd* transcriptional unit (Fig. 1e). We then similarly mapped the $Appl^d$ deletion and found that, unlike $Appl^{C2.1}$, it removes most of the intergenic region between *Appl* and *vnd* which possibly influences *vnd* function (Fig. 1e). We then assessed, by genetic complementation tests, if the different *Appl* null alleles possibly affected *vnd* function. We used vnd^A, a molecularly characterized lethal allele which impacts both the *vnd*-A and *vnd*-B transcripts (Fig. 2a; Haelterman et al. 2014). Although $Appl^{C2.1}/vnd^A$ transheterozygous MBs displayed no anatomical MB phenotypes, the $Appl^d/vnd^A$ and $Appl^{C1.4}/vnd^A$ MBs displayed 14% and 69% of β lobe absence, respectively (Fig. 2, b to d). Flies heterozygous for any of the 4 mutations individually displayed no MB phenotypes: $vnd^A/+$ ($n = 72$), $Appl^{C1.4}/+$ ($n = 60$), $Appl^{C2.1}/+$ ($n = 42$) and $Appl^d/+$ previously described (Soldano et al. 2013). Therefore, $Appl^d$ and $Appl^{C1.4}$, but not $Appl^{C2.1}$ affect *vnd* functions in MB development. We could write $Appl^d = Appl^{null}\ vnd^{weak}$, $Appl^{C1.4} = Appl^{null}\ vnd^{strong}$, and only $Appl^{C2.1} = Appl^{null}\ vnd^+$. In accordance with the genetic results, $Appl^d$ and $Appl^{C1.4}$ but not $Appl^{C2.1}$ individuals have a reduced Vnd protein expression (Supplementary Fig. 3). Taken together, these data strongly suggest that *vnd* is also involved in the MB β-branch axon growth and likely to a much greater extent than *Appl* itself.

Generation of new *vnd* CRISPR alleles deleted either for *vnd-B* or *vnd-A* function

The 2 *vnd* transcripts, *vnd*-A and *vnd-B*, produce 2 different Vnd proteins, respectively Vnd-A and Vnd-B (Fig. 2a). It was proposed that, while Vnd-A has its main role during embryogenesis, Vnd-B acts during metamorphosis (Stepchenko et al. 2011). To determine which Vnd isoform is required for MB β-branch axon growth, we produced the new *vnd* alleles $vnd^{C\Delta A}$ and $vnd^{C\Delta B}$ by CRISPR/Cas9 genomic engineering that eliminate either the *vnd*-A or the *vnd-B* isoform, respectively (Fig. 3a and Supplementary Fig. 4). We raised an anti-Vnd antiserum which recognizes both Vnd-A and Vnd-B proteins and found that indeed $vnd^{C\Delta A}$ and $vnd^{C\Delta B}$ individuals have a reduced Vnd expression (Supplementary Fig. 3). Males bearing a $vnd^{C\Delta B}$ mutant allele ($vnd^{C\Delta B}$/Y), as well as $vnd^{C\Delta B}/Appl^{C1.4}$ females, are viable and have essentially wild-type MBs (Fig. 3b). Males bearing a $vnd^{C\Delta A}$ mutant allele ($vnd^{C\Delta A}$/Y) are embryonic lethal similarly to other *vnd* null alleles which affect both isoforms. $Appl^{C1.4}/vnd^{C\Delta A}$ female MBs displayed a strong phenotype of β lobe absence with a penetrance (64%) like those of $Appl^{C1.4}/vnd^A$ female MBs (Fig. 4, a to d). We sought to determine the respective contribution of the lack of $Appl^+$ and the lack of vnd^+ for the strong β lobe absence in $Appl^{C1.4}/vnd^{C\Delta A}$ females. For this purpose, we added either a duplication of $Appl^+$ or a duplication of vnd^+ to this genotype. We found that $Appl^{C1.4}/vnd^{C\Delta A}$; *Dp*-$Appl^+$/+ females displayed 69% of β lobe absence, a penetrance not distinguishable from that observed without the duplication of wildtype *Appl* ($P = 0.42$). Therefore, in these 2 types of females ($Appl^{C1.4}/vnd^{C\Delta A}$; +/+ and $Appl^{C1.4}/vnd^{C\Delta A}$; *Dp*-$Appl^+$/+), the phenotype of β lobe absence seemed entirely due only to *vnd* lack-of-function. Indeed, $Appl^{C1.4}/vnd^{C\Delta A}$; +/+ females could be considered as $Appl^{null}\ vnd^{strong}/Appl^+\ vnd^{null}$ being homozygous mutant for *vnd* but heterozygous null for *Appl*. Similarly, $Appl^{C1.4}/vnd^{C\Delta A}$; *Dp*-$Appl^+$/+ females could be considered as $Appl^{null}\ vnd^{strong}/Appl^+\ vnd^{null}$; *Dp*-$Appl^+$/+ and are homozygous mutant for *vnd* but wild-type for *Appl*. Supporting the hypothesis of Vnd role in β axon growth, we observed a complete rescue when an extra dose of vnd^+ is supplied as in $Appl^{C1.4}/vnd^{C\Delta A}$; *Dp*-$vnd^+$/+ females (Fig. 4, a and d). $Appl^{C1.4}$/Y males have no $Appl^+$ function (null allele) and display reduced vnd^+ function. $Appl^{C1.4}$/Y male MB phenotype was moderately rescued by the presence of an extra dose of $Appl^+$ but strongly rescued by an extra dose of vnd^+ (Fig. 4, a and b). Similarly, $Appl^d$/Y males MB phenotype was rescued by both an extra dose of $Appl^+$ and by an extra dose of vnd^+ (Supplementary Fig. 5). $Appl^{C2.1}$/Y males MB phenotype was completely rescued by an extra dose of $Appl^+$ in accordance with $Appl^{C2.1}$ being $Appl^{null}\ vnd^+$ (Supplementary Fig. 5). Interestingly, $Appl^{C2.1}$/Y males MB phenotype was also rescued by an extra dose of vnd^+ (Supplementary Fig. 5). We comment this last result in the discussion. Taken together, these results strongly indicate that the *vnd*-A transcript but not the *vnd-B* transcript is specifically required for MB β-branch axon growth.

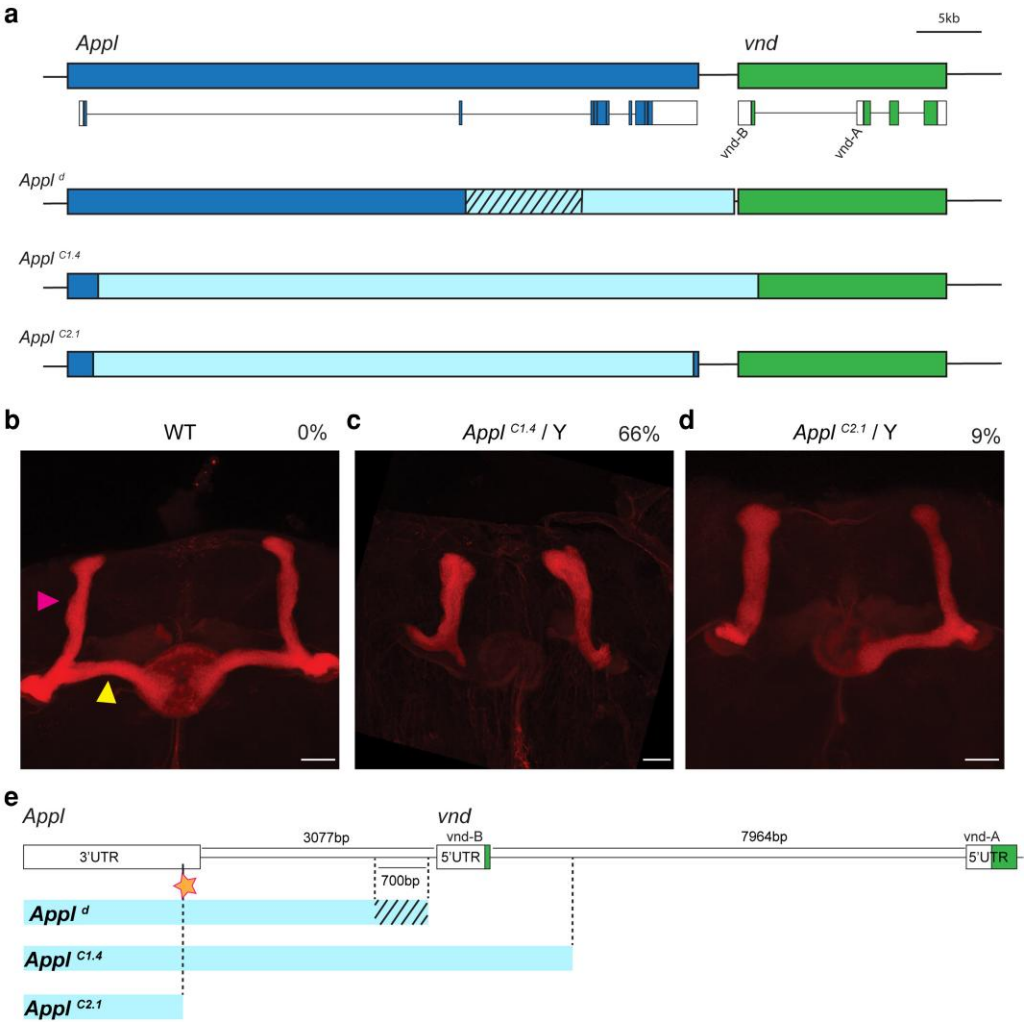

Fig. 1. Generating new *Appl* CRISPR/Cas9 alleles. a) Schematic representation of *Appl* (blue) and *vnd* (green) genes and transcripts. White boxes represent 5′UTR and 3′UTR, blue and green boxes represent *Appl* and *vnd* coding sequences, respectively. Schematic representations of the $Appl^{d}$, $Appl^{C1.4}$, and $Appl^{C2.1}$ mutant alleles where the deleted sequences are represented in light blue. The hatched black segment represents the uncertainty where the deletion of $Appl^{d}$ starts at its 5′end. b) Wild-type (WT) MB revealed by an anti-Fas2 staining. The pink and yellow arrowheads show respectively the α and β lobe ($n = 216$ MBs). c and d) Anti-Fas2 staining reveals the loss of β lobe on a representative $Appl^{C1.4}$ brain (66% $n = 147$ MBs) (c) and on $Appl^{C2.1}$ brain (9% $n = 253$ MBs) (d). The % represents the proportion of loss of β lobe for each genotype. Scale bar = 50 µm. Full genotypes: b) Canton-S. c) y $Appl^{C1.4}$ w^{1118}/Y. d) $Appl^{C2.1}$/Y. e) Representation of the 3′ limit of the $Appl^{d}$, $Appl^{C1.4}$ and $Appl^{C2.1}$ mutant alleles (light blue). The hatched black segment represents the uncertainty where the $Appl^{d}$ deletion ends in 3′. The orange star represents the position of the 3′ sgRNA used to create the 2 CRISPR/Cas9 deletions.

Vnd is expressed around the MBs and is not required within the MBs

To determine where *vnd* is expressed, we employed a *vnd-T2A-GAL4* line where GAL4 is under the control of endogenous *vnd* regulatory sequences via CRISPR gene targeting so that GAL4 and *vnd* are translated from a single mRNA transcript (Chen et al. 2015; Lee et al. 2020). UAS-GFP labeling revealed a pattern in the ventral ganglion of the third larval instar central nervous system (L3 CNS) similar to that described with immunostaining with antibodies against Vnd (Stepchenko et al. 2011) thus validating the use of the *vnd-T2A-GAL4* line as a bona fide *vnd* reporter (Supplementary Fig. 6). GFP was detected, in the developing brain, close to the MBs visualized by anti-Fas2 staining, from L3 to 24 h after puparium formation (APF) (Fig. 5, a to d′). Staining reveals a structure in the brain whose cell bodies are organized in a honeycomb pattern. To determine the identity of the cell bodies, we performed DAPI staining at the L3 stage. We observed a significant DAPI staining in these structures indicating that they correspond to cell nuclei (Fig. 5, e and e′). Moreover, these cell nuclei are Vnd positive and Repo negative (Fig. 5, f, f′ to g, g′) indicating that these cells correspond to neurons, rather than glia. The Vnd positive cells, inferred by the presence of GFP, were also Elav positive confirming their neuronal identity (Fig. 5, h to m). The neurites emanating from these cell nuclei are very close to the developing MB medial lobe from which the adult β lobe develops (Fig. 5, a to d′). Presently, we do not know the identity of the vnd^{+} neurons that flank the MBs. Noticeably, we did not observe any GFP labeling within the MBs themselves. This unexpected expression pattern suggests a non-cell-autonomous role for Vnd in the MB β-branch axon growth. We tested this hypothesis by MARCM mosaic analysis which allowed the generation of homozygous *vnd* loss-of-function MB clones in an otherwise heterozygous genetic background and overcame the homozygous lethality phenotype (Lee et al. 1999; Lee and Luo 1999). Mitotic recombination was induced in late-stage embryos/early first instar larvae and the clones were analyzed at the adult stage. We obtained 20 MB $vnd^{A/A}$ clones that include the αβ neurons. All the

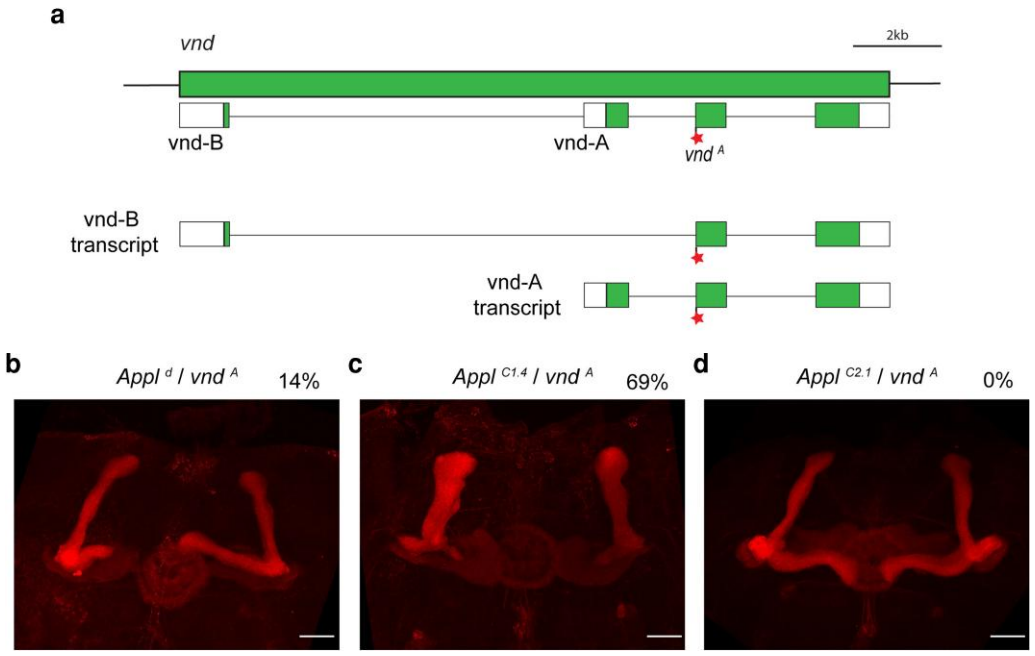

Fig. 2. $Appl^{d}$ and $Appl^{C1.4}$, but not $Appl^{C2.1}$, are impaired for *vnd* function. a) Schematic representation of *vnd* gene and transcripts. White boxes represent 5′ UTR and 3′UTR, green boxes represent coding sequences. Red star represents point mutation on vnd^{A} allele. Schematic representation of *vnd-B* and *vnd-A* transcripts. The vnd^{A} mutation affects both transcripts. b to d) Anti-Fas2 staining reveals the loss of β lobe on a representative $Appl^{d}/vnd^{A}$ brain (14% $n = 214$ MBs) (b), $Appl^{C1.4}/vnd^{A}$ brain (69% $n = 147$ MB) (c) but not on $Appl^{C2.1}/vnd^{A}$ brain (0% $n = 248$ MBs) (d). From the genetic complementation tests, we can write $Appl^{d} = Appl^{null}\ vnd^{weak}$, $Appl^{C1.4} = Appl^{null}\ vnd^{strong}$, and only $Appl^{C2.1} = Appl^{null}\ vnd^{+}$. The % represents the proportion of loss of β lobe for each genotype. Scale bar = 50 µm. Full genotypes: (b) $Appl^{d}$/y vnd^{A} w^{*} *FRT19A*. c) y $Appl^{C1.4}$ w^{1118}/y vnd^{A} w^{*} *FRT19A*. d) $Appl^{C2.1}$/y vnd^{A} w^{*} *FRT19A*.

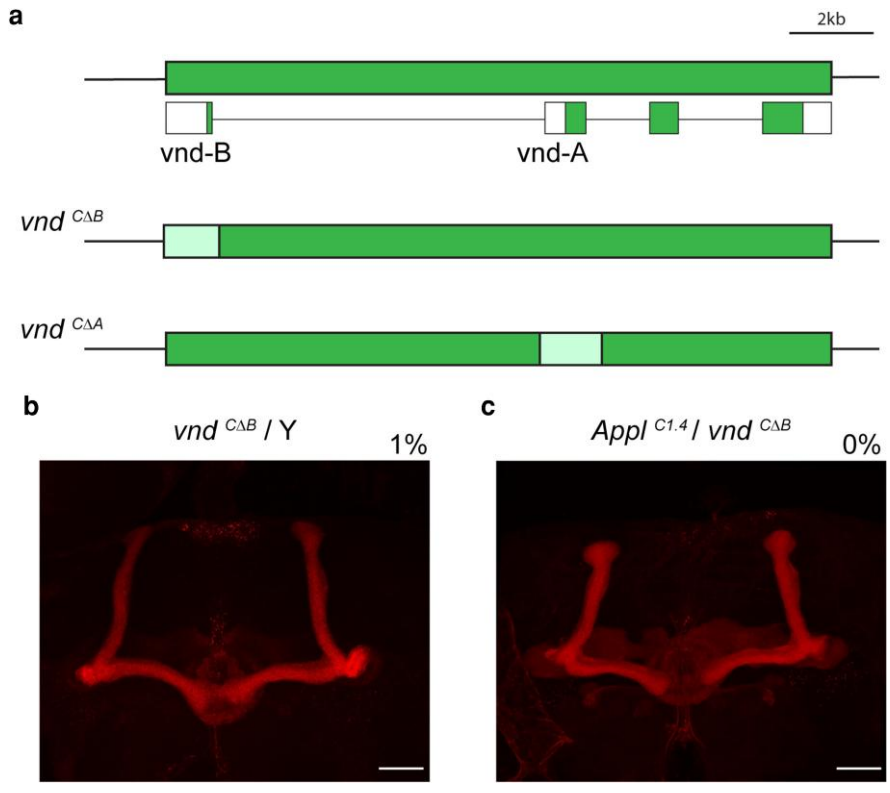

Fig. 3. Generating new *vnd* CRISPR alleles deleted either for the *vnd-B* or the *vnd-A* function. a) Schematic representation of *vnd* gene and transcripts. White boxes represent 5′UTR and 3′UTR, green boxes represent coding sequences. The deleted sequence region of $vnd^{C\Delta A}$ and $vnd^{C\Delta B}$ are represented in light green. b and c) Anti- Fas2 staining reveals essentially wild-type looking MBs on a representative $vnd^{C\Delta B}$ brain ($n = 146$ MBs) (b) and $Appl^{C1.4}/vnd^{C\Delta B}$ brain ($n = 159$ MB) (c). The % represents the proportion of loss of β lobe for each genotype. Scale bar = 50 µm. Full genotypes: b) y $vnd^{C\Delta B}$ w^{1118}/Y. c) y $Appl^{C1.4}$ w^{1118}/y $vnd^{C\Delta B}$ w^{1118}.

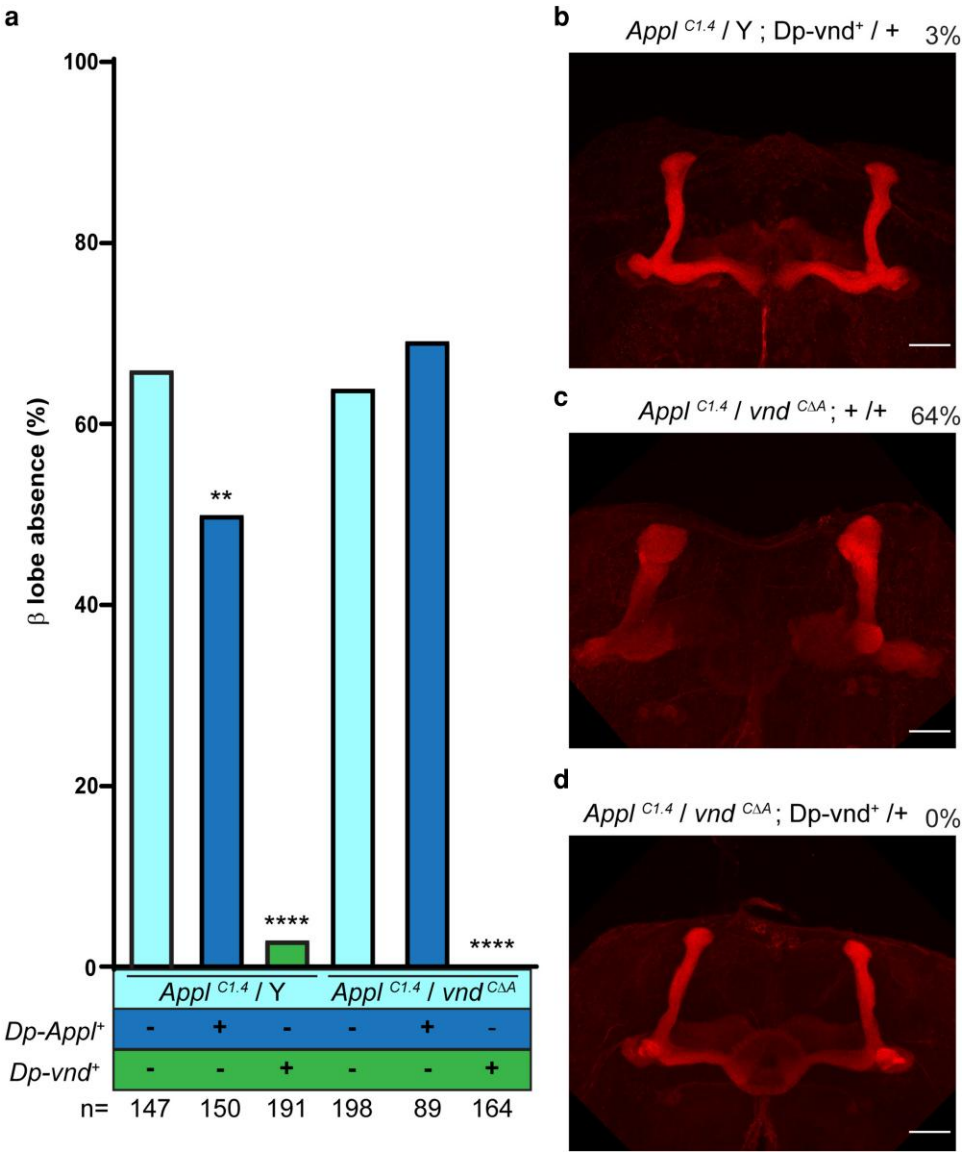

Fig. 4. Vnd-A is required for MB β-branch axon outgrowth. a) Quantitation of the rescue of MB β lobe absence of $Appl^{C1.4}$/Y (66%; $n = 147$ MBs, see a representative brain in Fig. 1c) and $Appl^{C1.4}/vnd^{C\Delta A}$ (64%; $n = 198$ MBs) (light blue) by an *Appl* duplication (dark blue) (50%; $n = 150$ MBs, 69%; $n = 89$ MBs) and by a *vnd* duplication (green) (3%; $n = 191$ MBs; 0%; $n = 164$ MBs). $^{**}P < 0.01$ and $^{****}P < 0.0001$. b to d) Anti-Fas2 staining on a representative rescued $Appl^{C1.4}$/Y; *Dp-vnd*$^+$/+ brain (b), $Appl^{C1.4}/vnd^{C\Delta A}$; +/+ brain (c) and on $Appl^{C1.4}/vnd^{C\Delta A}$; *Dp-vnd*$^+$/+ brain (d). The % represents the proportion of loss of β lobe for each genotype. Scale bar = 50 µm. Full genotypes: b) y $Appl^{C1.4}$ w^{1118}/Y; *Dp-vnd*$^+$/+. c) y $Appl^{C1.4}$ w^{1118}/y $vnd^{C\Delta A}$ w^{1118}; +/+. d) y $Appl^{C1.4}$ w^{1118}/y $vnd^{C\Delta A}$ w^{1118}; *Dp-vnd*$^+$/+.

20 *vnd* mutant clones displayed a β-branch axon growth that looked identical to that in wild-type clones (Supplementary Fig. 7). Moreover, we obtained similar results, namely normal β-branch axon growth, with 2 additional different null alleles, vnd^{A38} (8 clones) and vnd^{6} (4 clones) (Supplementary Fig. 7). Taken together, these results demonstrate that, although *vnd* function is strongly required for MB β-branch axon growth, *vnd* is neither required nor expressed in the MBs themselves. Therefore, it is most likely that Vnd regulates MB axon growth by a non-cell-autonomous mechanism.

The LTM loss of *Appl*-null flies is due to the absence of Appl in adult MBs

Although it is clear that *Appl* function is required for aversive olfactory memory, it has not yet been possible to assess the memory of *Appl*-null flies, because $Appl^{d}$ flies exhibit impaired electric shock avoidance (Luo et al. 1992; Bourdet et al. 2015). In such flies a defect in the aversive memory assay could result from an impairment in electric shock perception during conditioning and therefore not represent true memory defects. We showed here that $Appl^{d}$ also affects *vnd* function (Fig. 2b) and hence wondered if this impairment in electric shock avoidance was really due to the lack of the *Appl* function itself. In order to test this hypothesis, we evaluated the LTM performance of $Appl^{C2.1}$/Y flies which are null for *Appl* but wild-type for *vnd*. The electric shock avoidance and olfactory acuity appear wild-type in $Appl^{C2.1}$ flies (Fig. 6, a and b). Interestingly, $Appl^{C2.1}$ flies showed a complete loss of LTM, and this memory defect was fully rescued by the restricted expression of an *UAS-Appl* transgene in adult MBs (Fig. 6c). No rescue was detected in the non-induced 18 °C controls (Supplementary Fig. 8). These results conclusively demonstrate that the specific and complete loss of Appl affects LTM independently from any potential defects during brain development.

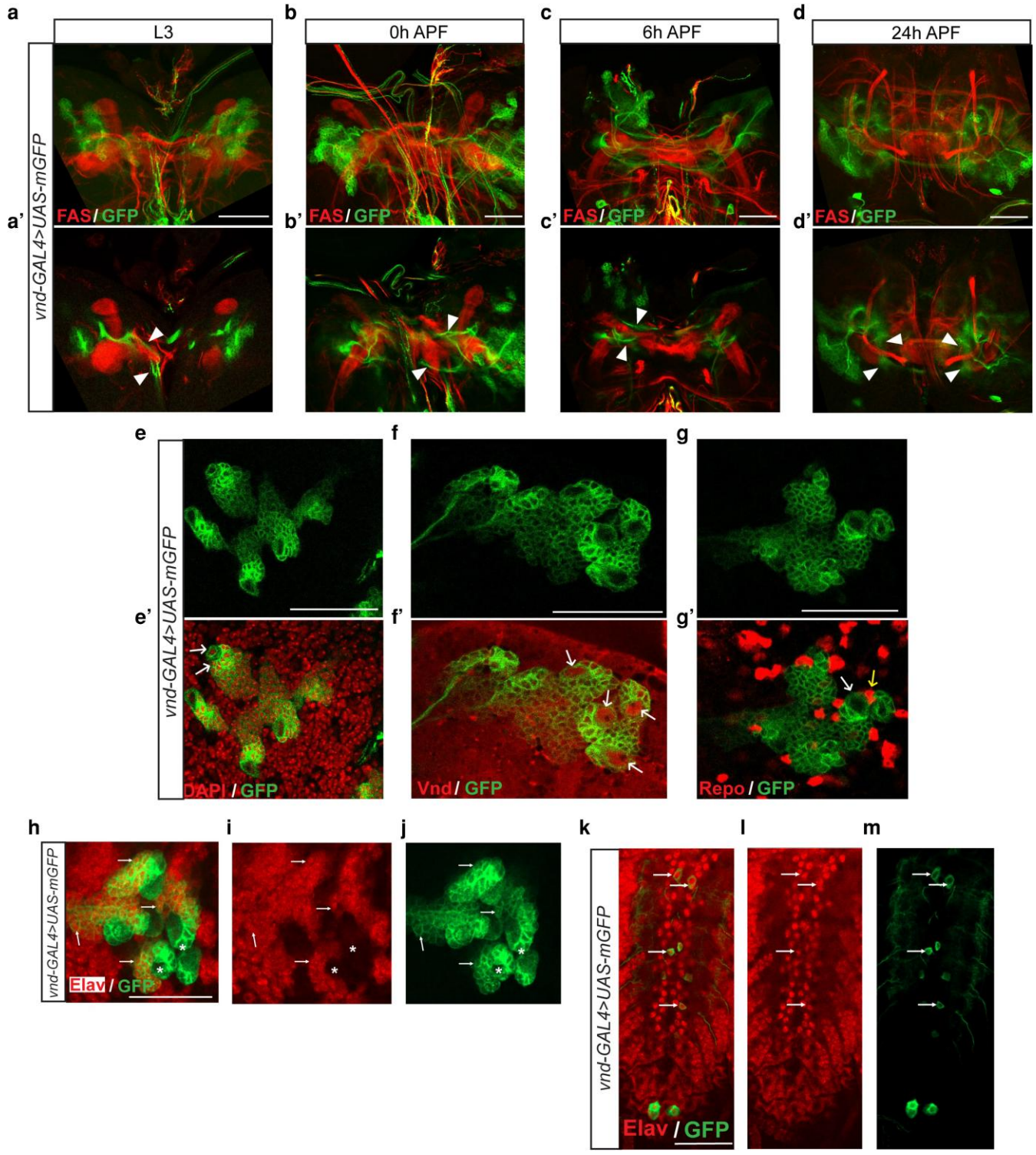

Fig. 5. *Vnd* is expressed close to the developing MB medial lobe. a to d′) Visualization of *vnd* expression in brain using *vnd-GAL4* driven *UAS-GFP* at L3, 0, 6, and 24 h APF. GFP was visualized on green and anti-FasII staining labeling of MB axons on red. Images in (a to d) are confocal z stacks taken the whole MB and images in (a′ to d′) are stacks of 5 sections from (a to d) respectively comprising GFP$^+$ regions surrounding MB. Arrowheads point to *vnd-GAL4* driven *UAS-GFP* neurites that surround MB medial lobes, which correspond to γ lobes from L3 to 6 h APF (a′ to c′) and β lobes at 24 h APF (d′). $n \geq 10$ for each time point. e to g′) are single confocal sections showing *vnd* expression using *vnd-GAL4* driven *UAS-GFP* (single channel) at L3. (e′ to be removed to g′) are merges of single channel (e to g) respectively and DAPI staining (red on e′), anti-vnd (red on f′) and anti-Repo (red on g′). DAPI labeled nuclei in GFP$^+$ cell bodies are pointed by arrows in e′. These nuclei were also Vnd positive (arrows in f′) but were not labeled by an anti-Repo (white arrow in g′) which labels glia nuclei (red dots pointed by a yellow arrow in g′) indicating that these Vnd positive nuclei belong to neurons. h to j) Visualization of a single confocal section of an L3 brain. h) Merged image of *vnd-GAL4* driven *UAS-GFP* (green) and anti-Elav (red), while (i) (anti-Elav, red) and (j) (GFP, green) show the individual channels. Elav labeling is observed in the nuclei of post-mitotic neurons (arrows), but is absent in neuroblasts and ganglion-mother-cell (asterisk). k to m) Visualization of a single confocal section of an L3 VNC. k) Merged image of *vnd-GAL4* driven *UAS-GFP* (green) and anti-Elav (red), while (l) (anti-Elav, red) and (m) (GFP, green) show the individual channels. Elav labeling is observed in the nuclei of Vnd expressing (GFP$^+$) post-mitotic neurons (arrows). Scale bars are 50 μm (a to g); 20 μm (h to j) and 40 μm (k to m). $n \geq 5$ brains for each type of staining. Full genotype: *vnd-T2A-GAL4 w**; 2 × *UAS-mGFP/+*.

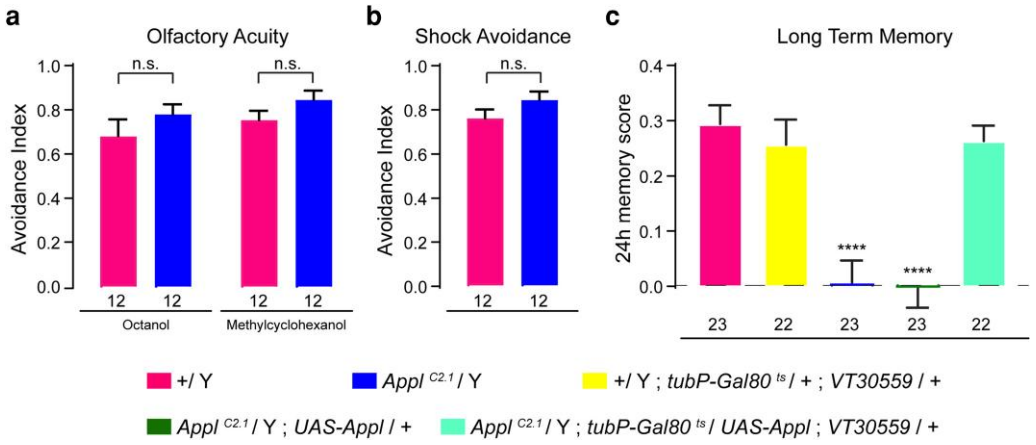

Fig. 6. The LTM defect of $Appl^{C2.1}$/Y flies is rescued by $Appl^{+}$ expression in the adult MB. a) Olfactory acuity was normal in $Appl^{C2.1}$/Y flies. For octanol, data presented as mean ± SEM. *t*-test $n = 12$, $t_{22} = 1.12$, $P = 0.26$, ns: not significant. For methylcyclohexanol, data presented as mean ± SEM. *t*-test $n = 12$, $t_{22} = 1.51$, $P = 0.15$, ns: not significant. b) Shock reactivity was normal in $Appl^{C2.1}$/Y flies. Data presented as mean ± SEM. *t*-test. $n = 12$, $t_{22} = 1.47$, $P = 0.16$, ns: not significant. c) Flies only null for *Appl* have no measurable LTM which is fully rescued by the restricted expression of *Appl* in adult MBs. Data presented as mean ± SEM. $n = 22$ to 23, $F_{(4, 108)} = 16{,}41$, $P < 0.0001$. Significance level of *t*-test or least significant pairwise comparison following ANOVA: $^{****}P < 0.0001$, ns: not significant.

Discussion

It was previously proposed that Appl is part of the membrane complex formed by the core PCP proteins Fz and Vang (Soldano et al. 2013). $Appl^{d}$ was, prior to this report, the only *Appl* null allele described. $Appl^{d}$ mutant flies completely lack Appl function and exhibit 14.5% MB β-lobe loss (Marquilly et al. 2021) in accordance with what has been reported (Soldano et al. 2013; Liu et al. 2021). This modestly penetrant axonal phenotype due to the lack of Appl could be due to partially redundant function provided by the other transmembrane receptors of the complex. Flies homozygous for the loss of function allele $Vang^{stbm\text{-}6}$ exhibit 50% β-lobe loss (Liu et al. 2021). As the $Appl^{d}$ allele involves complex chromosomic rearrangements (Luo et al. 1992), we leveraged CRISPR/Cas9 chromosomal engineering to produce a defined deletion of around 50 kb to specifically eliminate the *Appl* transcriptional unit. We recovered 2 *Appl* complete deletions (Fig. 1): $Appl^{C1.4}$ and $Appl^{C2.1}$ removing around 52 and 47 kb and exhibiting 66% and 9% β-lobe loss, respectively. DNA sequences analysis revealed that, while the $Appl^{C2.1}$ deletion removes only *Appl* sequences, the $Appl^{C1.4}$ deletion additionally removes a part of the proximally located transcriptional unit corresponding to the *vnd* gene (Fig. 1). This indicates that in addition to Appl, *vnd* is likely involved in the β-branch axon outgrowth. Moreover, as expected from the extent of the deletions and based on genetic complementation tests, the $Appl^{C1.4}$ deletion, but not the $Appl^{C2.1}$ deletion, affects *vnd* function. Most importantly, the $Appl^{d}$ deletion, which removes most of the Appl coding sequence and the intergenic region between *Appl* and *vnd*, also affects *vnd* function (Figs. 1 and 2).

The role of *vnd* in β-branch axon outgrowth is complicated by the fact that the viable *vnd* mutant alleles ($Appl^{d}$ and the $Appl^{C1.4}$ deletion), do not encode functional Appl. Nevertheless, employing a small (<100 kb) genomic $Appl^{+}$ duplication, we found that flies lacking only *vnd* function still exhibit 69% β-lobe loss and that this mutant phenotype is completely rescued by a small genomic vnd^{+} duplication (Fig. 4). This demonstrates a requirement of *vnd* function in MB β-branch axon outgrowth. To better understand the roles of both Vnd isoforms in the MB β-branch axon outgrowth, we produced 2 mutations, $vnd^{C\Delta B}$ and $vnd^{C\Delta A}$, which remove the *vnd-B* and the *vnd-A* transcript, respectively (Fig. 3 and Supplementary Fig. 4). *vnd-A* mRNA is expressed strongly in embryos and much less in larvae and adults contrarily to *vnd-B* mRNA (Stepchenko et al. 2011). It was therefore expected that the phenotype seen in adult MBs of pupal-born neurons should be due to *vnd-B* rather than *vnd-A*. Surprisingly, although Vnd-A has a significant role in MB axon growth, apparently Vnd-B plays very little to no role in this process. Noticeably, the MB phenotype of $Appl^{C1.4}/vnd^{C\Delta A}$ flies is similar in penetrance to that of $Appl^{C1.4}/vnd^{A}$ where vnd^{A} impacts both the *vnd-A* and *vnd-B* transcripts. This indicates that a lack of *vnd-A* function, and not that of vnd-B, underlies the β-branch axon outgrowth mutant phenotype.

If Vnd interacts with Appl within the MBs, we hypothesized that it might be expressed within the MBs, and act cell-autonomously like Appl. However, endogenous *vnd* transcription monitored by GAL4 expression that is translated from the same mRNA transcript and was validated by anti-Vnd staining did not reveal Vnd expression within the MBs. Rather, *vnd* is transcribed in cells within a neuronal brain structure near the developing MB medial lobe from which the adult β lobe develops (Fig. 5). Using MARCM mosaic analysis, we show that β axons extended from MB clones null for *vnd* function exhibit wild-type growth patterns (Supplementary Fig. 7) demonstrating a non-cell-autonomous requirement for Vnd. Therefore, we favor the hypothesis that *vnd* expressed in a MB surrounding brain structure causes the expression of 1 or more secreted factors regulating the axon growth of the developing β medial lobe. Given the position of the vnd^{+} neurons relative to the MBs during larval and pupal stages, we favor the hypothesis that these neurons signal locally to β lobe axons rather than over a long distance. Moreover, if Vnd is a transcriptional factor that produces the secreted ligand(s) necessary for the activation of the membrane multi-complex formed by Appl, Fz, and Vang, then a genetic interaction between Vnd and the complex can be expected. We hypothesize that the Vnd-Appl signaling pathway is the reason why $Appl^{C2.1}$/Y males MB phenotype is rescued by an extra dose of vnd^{+}. In 9% of the $Appl^{C2.1}$/Y MBs the axon growth of the developing β medial lobe is stopped. This means that in ∼90% MBs the mutant complex Fz-Vang, without the Appl protein, signals sufficiently to ensure normal axon growth. The 9% mutant phenotype is rescued to

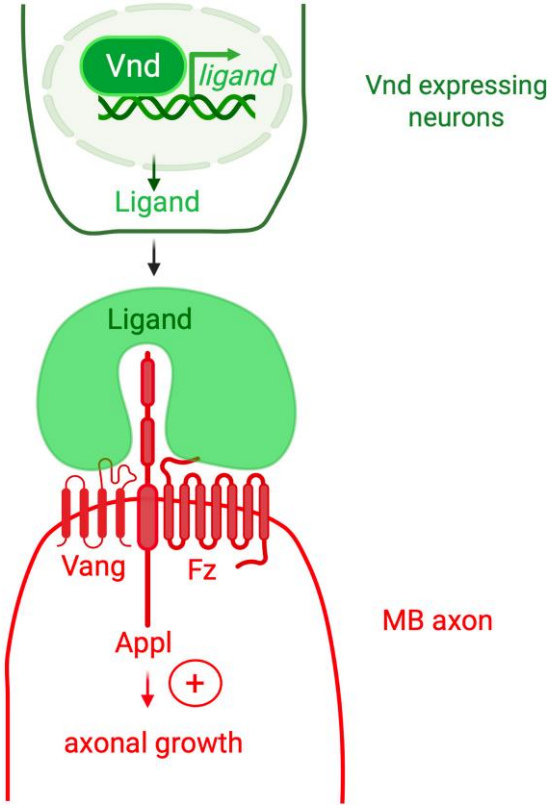

Fig. 7. Model for the activation of MB neuron axonal growth via the Vnd-Appl signaling pathway. Neurites emanating from Vnd-expressing neurons secrete a ligand necessary for the activation of a membrane multi-complex receptor formed by Vang-Appl-Fz within the MB axon growth cone. β-branch axon outgrowth requires activation of this complex receptor. Transcription of the ligand gene is upregulated by the Vnd transcription factor from the Vnd expressing neurons. This figure was created with BioRender.com. Boulanger, A. (2026) https://BioRender.com/azwjkeq.

2% when an extra dose of vnd^{+} is provided in individuals that are already wild-type for *vnd*. This vnd^{+} overexpression likely results in the production of extra ligand leading to more activation of the complex, formed by Fz and Vang but without Appl, promoting the rescue of the mutant phenotype. Our hypothesis that Vnd is compulsory for the activation of the multi-complex formed by Appl-Fz-Vang, necessary for the MB axon growth, is also a satisfactory explanation why the loss of Vnd has more impact on axon growth that the complete lack of Appl alone. A model of the Vnd-Appl signaling pathway is proposed (Fig. 7).

Prior to this study, it was not possible to evaluate the effects of a complete lack of *Appl* in aversive olfactory memory due to the failure of $Appl^{d}$ mutants to show normal shock reactivity (Luo et al. 1992; Bourdet et al. 2015). It was therefore hypothesized that it was the lack of Appl per se which was the cause of this impairment in electric shock avoidance. We reevaluated this hypothesis with the $Appl^{C2.1}$ allele which removes only the *Appl* function. $Appl^{C2.1}$/Y males react normally to electric shock and olfactory cues similarly to control flies but show a total lack of 24 h memory after a long-term conditioning regime (Fig. 6). Therefore, it is not the lack of *Appl* function in the $Appl^{d}$ mutants which underlies the impairment in electric shock avoidance. Importantly, the memory defect can be completely rescued by the expression of $Appl^{+}$ solely in the post-development adult MBs. This demonstrates that a complete lack of *Appl* results in a specific memory defect independently of any role that Appl might have in the developing brain. Consequently, the modest abnormal MB axonal growth morphological phenotype displayed by the $Appl^{C2.1}$ allele likely has no measurable impact on LTM. This is in accordance with the requirement of the vertical lobes but not the median lobes in aversive LTM (Pascual and Préat 2001).

The accumulation of amyloid-β (Aβ) is a hallmark feature of AD (Palop and Mucke 2010; Musiek and Holtzman 2015). Nevertheless, the production of Aβ peptides is at the expense of the full-length APP protein levels whose roles in AD are as yet, unclear. The *Drosophila* memory defect due to the complete lack of *Appl* may therefore be relevant to the memory defects associated with human AD. Interestingly, it was recently suggested that Appl extracellular domain supplies copper ions necessary for the catalytic activity of astrocyte-secreted superoxide dismutase 3 (Sod3), which generates H_2O_2 required for LTM formation in MBs (Rabah et al. 2025). Therefore, our observation that the memory defect resulting from the complete lack of *Appl* could be completely rescued by the expression of $Appl^{+}$ in the post-development MBs, thus bypassing any potential role of Appl in development, could be significant to our understanding of the physiological role of Appl, and possibly of human APP, in memory formation.

Data availability

Fly stocks used in this study are available from the Bloomington Drosophila Stock Center. The stocks generated in this study will be available soon from Bloomington and meanwhile they can be requested from the corresponding author. Imaging raw data are available from the corresponding author upon request.

Supplemental material available at GENETICS online.

Acknowledgments

We thank Aymeric Chartier (IGH, Montpellier) for fruitful discussions regarding the generation of the *Appl* CRISPR/Cas9 alleles. We thank the Bloomington *Drosophila* Stock Center (Indiana University), the BioCampus RAM-*Drosophila* facility and the BioCampus imaging facility MRI (Montpellier, France). We acknowledge BestGene and Genewiz for transgene service and DNA sequencing respectively. The 1D4 anti-Fasciclin II hybridoma, the 8D12 anti-Repo and the 9F8A9 anti-Elav monoclonal antibodies were obtained from the Developmental Studies Hybridoma Bank, created by the NICHD of the NIH and maintained at the University of Iowa, Department of Biology, Iowa City, IA 52242. We thank Chris Doe for the $vnd^{4\Delta38}$ and vnd^{6} alleles and Tzumin Lee for the *vnd-T2A-GAL4* line. Figure 7 was created with BioRender.com. Boulanger, A. (2026) https://BioRender.com/azwjkeq.

Funding

C.M. was supported by a PhD grant from the Ministère de l'Enseignement Supérieur et de la Recherche. C.M. and G.U.B. were supported by the Fondation pour la Recherche Médicale (FRM) respectively for the fourth PhD year and for a 3-yr post-doctoral fellowship. Work in the laboratory of J.-M.D. was supported by the Centre National de la Recherche Scientifique (CNRS), the Association pour la Recherche sur le Cancer (grants PJA 20151203422), the FRM (Programme "EQUIPES FRM2016" project DEQ20160334870) and the Agence Nationale de la Recherche (ANR-21-CE16-0033-ORIO to J.-M.D. and ANR-24-CE16-5161-ExOrion to A.B.). Work in the laboratory of T.P. was supported by the Fondation Langlois and the Fondation pour la Recherche Médicale (MND202411019909).

Conflicts of interest

The author(s) declare no conflicts of interest.

Literature cited

Aso Y *et al.* 2009. The mushroom body of adult *Drosophila* characterized by GAL4 drivers. J Neurogenet. 23:156–172. https://doi.org/10.1080/01677060802471718.

Boulanger A *et al.* 2011. ftz-f1 and Hr39 opposing roles on EcR expression during *Drosophila* mushroom body neuron remodeling. Nat Neurosci. 14:37–44. https://doi.org/10.1038/nn.2700.

Bourdet I, Preat T, Goguel V. 2015. The full-length form of the *Drosophila* amyloid precursor protein is involved in memory formation. J Neurosci. 35:1043–1051. https://doi.org/10.1523/JNEUROSCI.2093-14.2015.

Cassar M, Kretzschmar D. 2016. Analysis of amyloid precursor protein function in *Drosophila melanogaster*. Front Mol Neurosci. 9:61. https://doi.org/10.3389/fnmol.2016.00061.

Chen HM, Huang Y, Pfeiffer BD, Yao X, Lee T. 2015. An enhanced gene targeting toolkit for *Drosophila*: Golic+. Genetics. 199:683–694. https://doi.org/10.1534/genetics.114.173716.

Chu H, Parras C, White K, Jimenez F. 1998. Formation and specification of ventral neuroblasts is controlled by *vnd* in *Drosophila* neurogenesis. Genes Dev. 12:3613–3624. https://doi.org/10.1101/gad.12.22.3613.

de Tredern E *et al.* 2021. Glial glucose fuels the neuronal pentose phosphate pathway for long-term memory. Cell Rep. 36:109620. https://doi.org/10.1016/j.celrep.2021.109620.

Doudna JA, Charpentier E. 2014. Genome editing. The new frontier of genome engineering with CRISPR-Cas9. Science. 346:1258096. https://doi.org/10.1126/science.1258096.

Haelterman NA *et al.* 2014. Large-scale identification of chemically induced mutations in *Drosophila melanogaster*. Genome Res. 24:1707–1718. https://doi.org/10.1101/gr.174615.114.

Jiménez F *et al.* 1995. Vnd, a gene required for early neurogenesis of *Drosophila*, encodes a homeodomain protein. EMBO J. 14:3487–3495. https://doi.org/10.1002/j.1460-2075.1995.tb07355.x.

Lee T, Lee A, Luo L. 1999. Development of the *Drosophila* mushroom bodies: sequential generation of three distinct types of neurons from a neuroblast. Development. 126:4065–4076. https://doi.org/10.1242/dev.126.18.4065.

Lee T, Luo L. 1999. Mosaic analysis with a repressible cell marker for studies of gene function in neuronal morphogenesis. Neuron. 22:451–461. https://doi.org/10.1016/S0896-6273(00)80701-1.

Lee YJ *et al.* 2020. Conservation and divergence of related neuronal lineages in the *Drosophila* central brain. Elife. 9:e53518. https://doi.org/10.7554/eLife.53518.

Leyssen M *et al.* 2005. Amyloid precursor protein promotes post-developmental neurite arborization in the *Drosophila* brain. EMBO J. 24:2944–2955. https://doi.org/10.1038/sj.emboj.7600757.

Lin S. 2023. The making of the *Drosophila* mushroom body. Front Physiol. 14:1091248. https://doi.org/10.3389/fphys.2023.1091248.

Liu T *et al.* 2021. The amyloid precursor protein is a conserved Wnt receptor. Elife. 10:e69199. https://doi.org/10.7554/eLife.69199.

Luo L, Tully T, White K. 1992. Human amyloid precursor protein ameliorates behavioral deficit of flies deleted for Appl gene. Neuron. 9:595–605. https://doi.org/10.1016/0896-6273(92)90024-8.

Marquilly C *et al.* 2021. Htt is a repressor of Abl activity required for APP-induced axonal growth. PLoS Genet. 17:e1009287. https://doi.org/10.1371/journal.pgen.1009287.

Martin-Morris LE, White K. 1990. The *Drosophila* transcript encoded by the β-amyloid protein precursor-like gene is restricted to the nervous system. Development. 110:185–195. https://doi.org/10.1242/dev.110.1.185.

McGuire SE, Le PT, Osborn AJ, Matsumoto K, Davis RL. 2003. Spatiotemporal rescue of memory dysfunction in *Drosophila*. Science. 302:1765–1768. https://doi.org/10.1126/science.1089035.

Musiek ES, Holtzman DM. 2015. Three dimensions of the amyloid hypothesis: time, space and 'wingmen'. Nat Neurosci. 18:800–806. https://doi.org/10.1038/nn.4018.

Nicolas M, Hassan BA. 2014. Amyloid precursor protein and neural development. Development. 141:2543–2548. https://doi.org/10.1242/dev.108712.

Palop JJ, Mucke L. 2010. Amyloid-β-induced neuronal dysfunction in Alzheimer's disease: from synapses toward neural networks. Nat Neurosci. 13:812–818. https://doi.org/10.1038/nn.2583.

Pascual A, Préat T. 2001. Localization of long-term memory within the *Drosophila* mushroom body. Science. 294:1115–1117. https://doi.org/10.1126/science.1064200.

Placais PY *et al.* 2017. Upregulated energy metabolism in the *Drosophila* mushroom body is the trigger for long-term memory. Nat Commun. 8:15510. https://doi.org/10.1038/ncomms15510.

Port F, Chen HM, Lee T, Bullock SL. 2014. Optimized CRISPR/Cas tools for efficient germline and somatic genome engineering in *Drosophila*. Proc Natl Acad Sci U S A. 111:E2967–E2976. https://doi.org/10.1073/pnas.1405500111.

Rabah Y *et al.* 2025. Astrocyte-to-neuron H_2O_2 signalling supports long-term memory formation in *Drosophila* and is impaired in an Alzheimer's disease model. Nat Metab. 7:321–335. https://doi.org/10.1038/s42255-024-01189-3.

Selkoe DJ, Hardy J. 2016. The amyloid hypothesis of Alzheimer's disease at 25 years. EMBO Mol Med. 8:595–608. https://doi.org/10.15252/emmm.201606210.

Soldano A *et al.* 2013. The *Drosophila* homologue of the amyloid precursor protein is a conserved modulator of Wnt PCP signaling. PLoS Biol. 11:e1001562. https://doi.org/10.1371/journal.pbio.1001562.

Soldano A, Hassan BA. 2014. Beyond pathology: APP, brain development and Alzheimer's disease. Curr Opin Neurobiol. 27:61–67. https://doi.org/10.1016/j.conb.2014.02.003.

Stepchenko AG, Pankratova EV, Doronin SA, Gulag PV, Georgieva SG. 2011. The alternative protein isoform NK2B, encoded by the vnd/NK-2 proneural gene, directly activates transcription and is expressed following the start of cells differentiation. Nucleic Acids Res. 39:5401–5411. https://doi.org/10.1093/nar/gkr121.

Tully T, Quinn WG. 1985. Classical conditioning and retention in normal and mutant *Drosophila melanogaster*. J Comp Physiol A. 157:263–277. https://doi.org/10.1007/BF01350033.

Editor: J. Wildonger